

DANISH METEOROLOGICAL INSTITUTE

SCIENTIFIC REPORT

03-02

**Geometrical Optics Phase
Matching of Radio Occultation Signals**

By

**A.S. Jensen, M.S. Lohmann, H.-H. Benzon,
and A.S. Nielsen**



COPENHAGEN 2003

ISSN-Nr. 0905-3263
ISSN-Nr. 1399-1949 (Online)
ISBN-Nr. 87-7478-473-0

Geometrical Optics Phase Matching of Radio Occultation Signals

Abstract

A. S. Jensen (1), M. S. Lohmann (1), H.-H. Benzon (1),
A. S. Nielsen (1).

Remote measurements of the state of the atmosphere can be done by radio occultation between satellite links, a GPS satellite transmitting a radio signal to a receiving low earth orbit satellite (LEO), or between a LEO-LEO satellite constellation. The bending angle of the traversing optical ray can be measured by detecting the Doppler shift of radio signals. The bending angle is an integrated measure of the refractive index in the atmosphere traversed by the optical ray. With a time series of the bending angle, it is possible to perform an inversion to reveal the refractive index. Various techniques for the retrieval of the bending does already exist. The most recent methods have solved the problem of multipath, i.e., when the atmosphere allows several rays to exist simultaneously. In this report, a new phase matching technique of radio occultation signals will be presented.

Introduction

In general terms, the radio occultation technique is based on the bending of radio waves caused by refractive index gradients in a planetary atmosphere [e.g. *Kursinski et al.*, 1997, 2000]. In Global Navigation Satellite System (GNSS) radio occultations, the bending is measured as radio waves traversing the Earth's atmosphere from a GNSS satellite to a Low Earth Orbit (LEO) satellite. Traditionally this is done by measuring the Doppler shift of the radio wave from which the impact parameter can be retrieved and subsequently the bending angle with the knowledge of the positions and the velocities of the satellites. The retrieved pairs of bending angle and impact parameter can be inverted through the Abel transform to yield the index of refractivity as function of height [*Fjeldbo et al.*, 1971].

The propagating radio waves can be described as rays according to geometrical optics when diffraction effects in the refractive media can be neglected. This excludes media where optical turbulence is present, areas with very strong gradient in the refractive index, and areas near surfaces. In general the geometrical optical description will be adequate when the disturbances in the media are much smaller than the wavelength.

A receiver can detect one or more rays emerging from a transmitter. In single ray regions, the computation of bending angles is straightforward as they are unambiguously related to the instantaneous frequency of the received signal. Therefore, radio occultation measurements have conventionally been based on the instantaneous frequency. However, radio signals propagating through the lower troposphere may have a very complex structure due to multipath effects caused mainly by water vapour structures [*Gorbunov et al.*, 1996; *Gorbunov and Gurvich*, 1998; *Gorbunov et al.*, 2000; *Sokolovskiy*, 2001]. In regions that exhibit multipath, the bending angles cannot be derived directly from the instantaneous frequency of the measured signal because the instantaneous frequency will be related, not to a single pair of bending angle and impact parameter, but to two or more pairs. Another drawback of retrieving the bending angle directly from the

instantaneous frequency is that the vertical resolution is limited by the size of the Fresnel zone. Thus, there has been much effort in developing techniques with high vertical resolution that are capable of correctly retrieving the bending angle profile in multipath regions [Gorbunov, 2001]. So far, five high resolution methods have been proposed for processing of radio occultation signals in multipath regions: (1) back-propagation [Gorbunov et al., 1996; Hinson et al., 1997, 1998; Gorbunov and Gurvich, 1998], (2) radio-optics, [Lindal et al., 1987; Pavelyev, 1998; Hocke et al., 1999; Sokolovskiy, 2001; Gorbunov, 2001], (3) Fresnel diffraction theory [Marouf et al., 1986; Mortensen and Høeg, 1998; Meincke, 1999], (4) canonical transform [Gorbunov, 2001], and (5) the Full Spectrum Inversion (FSI) method [Jensen et al., 2003].

This report presents a new high-resolution radio-holographic method, which shortly can be described as a phase matching or a transform of the occultation signal. The method can be described in general terms, but the use of the method can only be done with an explicit matching phase function. Here two explicit or special forms of the phase function are considered. In the first form, the method is identical to the FSI method [Jensen et al., 2003], and the second form is a model derived from the geometrical optical phase in vacuum. It will be shown, that this model of the phase transform has the same high-resolution properties as the FSI method, but solves some minor problems related to defocusing.

The outline for the report is as follows: First, the general phase matching method is presented, and a special case is analysed in a spherical symmetric atmosphere.

The Phase Matching

In the following, the general theory for the phase matching will be established. The main point here is to use the stationary phase method [Born and Wolf, 1999] to evaluate the resulting phase transform. There are two main constrains for using the stationary phase method in this context: (1) The amplitude of the integrant must be slowly varying compared to the second order derivative of the phase of the integrant, and (2) one and only one stationary point must be present. Given a complex (radio occultation) signal, $f(t) = \sum A_i(t)e^{i\psi_i(t)}$, we can define a phase transform as follows:

$$u(c) = \sum \int_0^T A_i(t)e^{i\psi(t)-i\psi_o(c,t)} dt, \quad (1)$$

where the phase $\psi_o(c,t)$ is a function of time t , the parameter c defines the transform space. The parameter c can in principle take all values. Eq.1 can be generalized by considering the parameter c as a vector. In addition, associated with the phase, an (slowly varying) amplitude factor could be used; this will be done later. The occultation signals are in general a sum of signals, which accounts for multipath. In the following, the summation will be omitted and the signal used should be perceived as one of the signals in the sum. The phase matched function $u(c)$ can be brought on an explicit form if the signal fulfill the constrains given in (1) and (2), as stated above. It yields

$$\begin{aligned}
u(c) &= \int_0^T A(t) e^{i(\psi(t) - \psi_o(c,t))} dt = \\
& \int_0^T A(t) e^{i(\psi(t_1) - \psi_o(c,t_1)) + i(\dot{\psi}(t_1) - \dot{\psi}'_o(c,t_1))(t-t_1) + \frac{1}{2}(\ddot{\psi}(t_1) - \ddot{\psi}''_o(c,t_1))(t-t_1)^2 + \dots} dt \cong \\
& \sqrt{\frac{2\pi i}{\dot{\psi}(t_1) - \dot{\psi}'_o(c,t_1)}} A(t_1) e^{i(\psi(t_1) - \psi_o(c,t_1))} \Big|_{\dot{\psi}(t_1) = \dot{\psi}'_o(c,t_1)}.
\end{aligned} \tag{2}$$

All derivatives here are with respect to time. The condition $\dot{\psi}(t_1) = \dot{\psi}'_o(c,t_1)$ determines the stationary point(s) from which $c = c(t_1)$ can be found. It is assumed that only one solution exist according to condition (2) above. The phase in Eq.2, $\psi(t_1) - \psi_o(c,t_1)$, is a function of the transforming space parameter c , and by differentiation of the phase with respect to c , an auxiliary function on parametrical form can be found:

$$\left[c, -\frac{\partial \psi_o}{\partial c} \right] \tag{3}$$

which express a relation between the transform space parameter and the partial derivative of the matching phase.

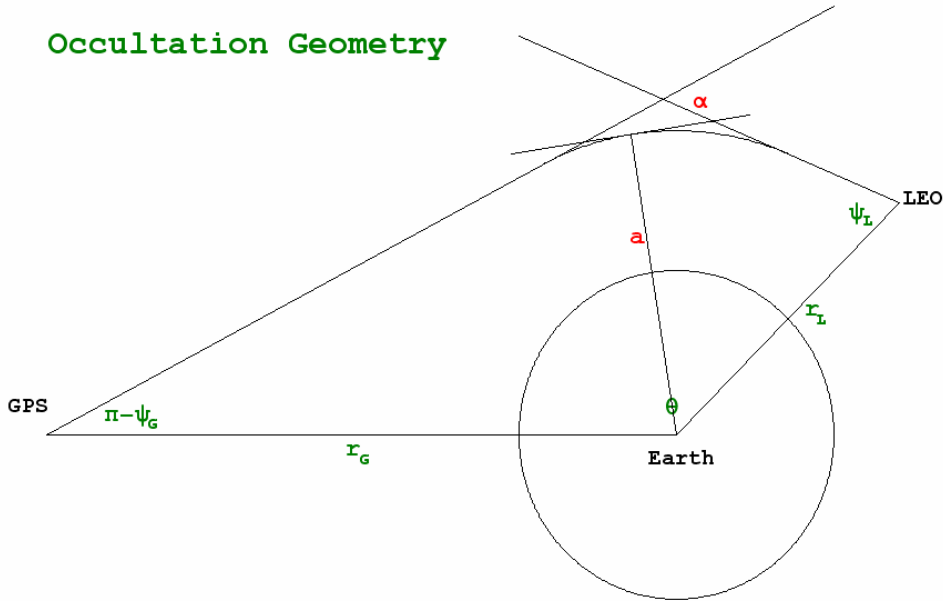


Figure 1: Occultation Geometry

The figure has been sketched with the use of Eq.4, which can be considered as an approximation to the geometrical optics ray path. α is the bending angle, ψ_G, ψ_L the angles between the ray path and the radius vector at the GPS and LEO positions, θ is the angle between the LEO and GPS, r_G, r_L the distance to the Earth center from the GPS and LEO and a is the impact parameter, respectively. As noticed, the angles are connected by the relation: $\alpha = \theta + \psi_L - \psi_G$.

The formulas derive here can be used to design some wanted properties of the match, by knowing the structure of the signal phase. This will not be done here systematically, but instead some examples of this will be elaborated. A special case is here the FSI method, where the transforming phase is given by $\psi_o(\mathbf{c}, t) = ct$, i.e., the phase matching becomes the Fourier transform, and the auxiliary function $[c, -t_1]$ (Eq.3) gives the Doppler frequency as function of time. Another special case is to let the auxiliary function take the form $[c, -k\beta]$. Here c is the impact parameter, β is the bending angle and k is the wavenumber. The matching phase yields in this case for a spherical symmetric atmosphere:

$$\psi_o(c, t) = k(\sqrt{r_L^2 - c^2} + \sqrt{r_G^2 - c^2}) + c\beta. \quad (4)$$

where r_G and r_L are the radii of the GPS and LEO satellites, respectively. It is seen that the auxiliary function $[c, -k\beta]$ can be found by using Eq.3. The bending angle β is related to the parameter c and the mutual angle θ between the GPS and the LEO satellites by the standard relation:

$$\beta = \theta - A \tan\left(\frac{\sqrt{r_L^2 - c^2}}{c}\right) - A \tan\left(\frac{\sqrt{r_G^2 - c^2}}{c}\right). \quad (5)$$

The notation for the impact parameter and the bending angle (\mathbf{c}, β) is used in order to distinguish these forced parameters from the real quantities (\mathbf{a}, α) , which all over in this report are associated to the real occultation signals.

The phase in Eq.4 is actually an approximation to the optical ray path. The idea to the form (Eq.4) comes from an analysis of the occultation phase with a spherical symmetric refraction profile: The optical phase can in this case be expressed as:

$$\psi = k\sqrt{r_L^2 - a^2} + k\sqrt{r_G^2 - a^2} + ka\alpha - 2\int_a^\infty \sqrt{u^2 - a^2} \frac{d\ln(n)}{du} du \quad (6)$$

where a is the impact parameter and α the bending angle. By setting $n = 1, a = c$ and $\alpha = \beta$ the expression above turns formally into Eq.4.

The stationary point determined by $\dot{\psi}(t_1) = \dot{\psi}_o(\mathbf{c}, t_1)$ can explicitly be expressed by:

$$\dot{\psi}(t_1) - \dot{\psi}_o(c, t_1) = k(\dot{r}_L \sqrt{1 - \frac{a^2}{r_L^2}} + \dot{r}_G \sqrt{1 - \frac{a^2}{r_G^2}} + a\dot{\theta} - \dot{r}_L \sqrt{1 - \frac{c^2}{r_L^2}} + \dot{r}_G \sqrt{1 - \frac{c^2}{r_G^2}} + c\dot{\theta}) \quad (7)$$

The solution of this is simply, $c = a$ which verifies that with the phase given in Eq.4 the result of the phase match gives the bending angle as function of impact parameter. Using Eqs.4 and 6 to compute the phase difference at the stationary point yields;

$$\psi(t_1) - \psi_0(c, t_1)|_{a=c} = -2k \int_c^{\infty} \sqrt{u^2 - c^2} \frac{d \ln(n)}{du} du. \quad (8)$$

Differentiating the difference phase with respect to the parameter c then gives the bending angle multiplied by the wavenumber, as predicted above.

Now, to finish the interpretation of this phase matching technique, the equivalent matching amplitude has to be calculated. This is done in Appendix I, together with an analysis of the benefits of using amplitude in the phase matching. The result from Appendix I, shows that the use of the phase in Eq.4 cancels the defocusing factor perfect, which together with the amplitude function makes the output amplitude of the phase transform $u(c)$ a constant in the absence of absorption in the atmosphere. This last property is the main advantage of the method compared to the FSI method.

The phase matching method related to the Fourier Integral Operators (FIO) method used in the canonical transform method developed by [Gorbunov et al, 2002] and classified as canonical transform without back propagation. In this, the differential equations for the specialized case mentioned above, has been stated, but no solutions has been given. The connection between the method described here and the method of [Gorbunov et al, 2002] has been discovered in a private communication. Both methods rely on the synthetic antenna concept and the method of the stationary phase used in the FSI method.

Now, this interpretation of the geometrical optic phase matching technique has been rather lengthy, so a short recap of the practical use of the method is appropriate.

1: The phase matching is performed on the occultation signal:

$$\begin{aligned} u(c) &= \int_0^T A(t) e^{i\psi(t)} C(t) e^{-\psi_o(c,t)} dt \\ &\cong \sqrt{P_G} e^{i((\psi(t_1) - \psi_o(c,t_1) + \pi/2))} \Big|_{\psi(t_1) = \psi_o(c,t_1)}, \end{aligned}$$

2: The phase is differentiated with respect to c giving the bending angle.

$$\frac{d}{dc} (\psi(t_1) - \psi_o(c, t_1)) \Big|_{\psi(t_1) = \psi_o(c, t_1)} = k\beta$$

3: The result $[c, \beta]$ is Abel transformed giving the refractive index.

The number of c values used, will depend on the magnitude of the bending angle in that respect that the phase variation should be sufficiently small so the differentiation is correct.

Conclusion

The technique of geometrical optical phase matching introduced here is a specialization of the previous developed FSI method taking the form of the optical phase into account. Both methods utilize the synthetic aperture formed by the moving LEO satellite to give a high resolution of the measured impact parameter and both rely on the method of stationary phase. Initial simulations of the phase matching technique show no advantage compared to the FSI method, which is to be expected, as long as the task is to determine the bending angle as function of the impact parameter. However, if absorption can be measured, as proposed by [Lohmann *et al.*, 2003], the phase matching technique will have a clear advantage. In the practical use of the methods, i.e., with respect to computation time, the phase matching method is much slower than the FSI method. The FSI method uses a FFT for the computation of the spectrum, which not is possible with the phase matching case.

Appendix I: Calculation of the amplitude factor in the geometrical optics phase match.

The amplitude factor in the phase matching method can partly be defined arbitrarily as long as it is slowly varying. However, it is convenient to use an amplitude factor, which makes the amplitude of the phase match constant. Using Eq.2 and the geometric optical intensity [Leroy, 2001], [Jensen et al., 2003]. The intensity yields:

$$I_L = \frac{P_G}{2\pi} \frac{a}{r_G r_L \sin(\theta_L) \sqrt{r_G^2 - a^2} \sqrt{r_L^2 - a^2} \left(\frac{d\theta}{da}\right)_L} \quad (\text{Al.1})$$

where P_G is the intensity at the transmitting GPS satellite and $(d\theta/da)_L$ the defocusing factor at the receiving LEO satellite. The defocusing factor can be approximated to yield $(d\theta/da)_L \approx \dot{\theta}/\dot{a}$.

The second time derivative of the phase in Eq. 1 can be expressed as:

$$\ddot{\psi}(t_1) - \ddot{\psi}_o(c, t_1)|_{a=c} = k\dot{a} \left(\dot{\theta} - \frac{a\dot{r}_L}{r_L \sqrt{r_L^2 - a^2}} - \frac{a\dot{r}_G}{r_G \sqrt{r_G^2 - a^2}} \right) \quad (\text{Al.2})$$

In Eq.A1.2 it is seen that the defocusing factor $((d\theta/da)_L \approx \dot{\theta}/\dot{a})$ is a multiplicative factor, which means that the defocusing is perfectly canceled out in the phase transform. This property is the main advantage of the geometrical optics phase match method compared with the FSI method, where a perfect cancellation only is present when the radial velocities are zero. Since other variations in the amplitude are slow, it is then possible to assign an amplitude factor to the phase match, which gives constant amplitude in the transformed space. Besides the beauty of this, it has the function that it can reveal and detected absorptions along the ray path [Lohmann et al., 2003].

By defining the matching amplitude as follows

$$C(c, t) = \sqrt{\sin(\theta) \dot{\theta} \left(\frac{r_L r_G}{c} \sqrt{r_G^2 - c^2} \sqrt{r_L^2 - c^2} \dot{\theta} - \dot{r}_L r_G \sqrt{r_G^2 - c^2} - \dot{r}_G r_L \sqrt{r_L^2 - c^2} \right)}, \quad (\text{Al.3})$$

this purpose is realized.

References

- Born, M. and E. Wolf, Principles of Optics, Cambridge University Press, 1999.
- Fjeldbo, G., A. J. Kliore, and R. Eshlermann, The neutral atmosphere of Venus Studied with the Mariner V radio occultation experiments, *Astron. J.*, 76(2), 123-140, 1971.
- Gorbunov, M. E., S. V. Sokolovskiy, and L. Bengtson, Advanced algorithms of inversion of GPS/MET satellite data and their application to reconstruction of temperature and humidity Tech. Rep Report No. 211, Max Planck Institute for Meteorology, Hamburg, 1996.
- Gorbunov, M. E. and A. S. Gurvich, Microlab-1 experiment: Multipath effects in the lower troposphere. *J. Geophys. Res.*, 103(D12), 13,819-826, 1998.
- Gorbunov, M. E., A. S. Gurvich, and L. Kornblueh, Comparative analysis of radioholographic methods of processing radio occultation data, *Radio Sci.*, 35(4), 1025-1034, 2000.
- Gorbunov, M. E., Radioholographic methods for processing radio occultation data in multipath regions, *Scientific Report 01-02*, Danish Meteorological Institute, Copenhagen, 2001.
- Gorbunov, M. E. Lauritsen, K. B. Canonical Transform Methods for Radio Occultation Data, *Scientific Report 02-10*, Danish Meteorological Institute, Copenhagen, 2002.
- Hinson, D. P., F. M. Flasar, A. J. K. P. J. Schinder, J. D. Twicken, and R. G. Herrera, Jupiter's Ionosphere: Results from the first Galileo radio occultation experiment, *Geophys. Res. Lett.*, 24(17), 2107-2110, 1997.
- Hinson, D. P., J. D. Twicken, and E. T. Karayel, Jupiter's Ionosphere: New Results from the first Voyager2 radio occultation measurements, *J. Geophys. Res.*, 103(A5), 9505-9520, 1998.
- Hocke, K. A., A. G. Pavelyev, O. I. Yakovlev, L. Barthes, and N. Jakowski, Radio occultation data analysis by the radioholographic method, *J. Atmos. Sol. Terr. Phys.*, 61(15) 1169-117, 1999.
- International Telecommunication Union, Propagation in non-ionized media, *J. Comp. Phys.*, 41, 115-131, 1981.
- Kursinski, E. R., G. A. Hajj, J. T. Schofield, and R. P. Linfield, Observing Earth's Atmosphere with Radio Occultation Measurements using Global Positioning System. *J. Geophys. Res.*, 102,(D19), 23,429-465, 1997.
- Kursinski, E. R., G. A. Hajj, S. S. Leroy, and B. Herman, The GPS Radio Occultation Technique. *TAO*, 11(1), 53-114, 2000.
- Leroy, S. S., Amplitude of an occultation signal in three dimensions, submitted to *Radio Science*, 2001.
- Lindal, G. F., J. R. Lyons, D. N. Sweetnam, V. R. Eshleman, D. P. Hinson, and G. L. Tyler, The atmosphere of Uranus: Results of radio occultation measurements with Voyager 2, *J. Geophys. Res.*, 92(A13), 14,987-001, 1987.
- Lohmann, M. S., A. S. Jensen, H.-H. Benzon, A. S. Nielsen, *Computation of atmospheric absorption by the FSI technique*, in preparation, 2003.
- Marouf, E. A., G. L. Tyler, and P. A. Rosen, Profiling Saturn rings by radio occultation. *ICARUS*, 68, 120-166, 1986.
- Meincke, M. D., Inversion methods for atmospheric profiling with GPS occultations. *Scientific Report 99-11*, Danish Meteorological Institute, Copenhagen, 1999.
- Mortensen, M. D. and P. Høeg, Inversion of GPS occultation measurements using Fresnel diffraction theory. *Geophys Res. Letters*, 25(13), 2446-2449, 1998.
- Pavelyev, A. G., On the feasibility of radioholographic investigations of wave fields near the Earth's radio-shadow zone on the satellite-to-satellite path, *J. Commun Technol. Electron.*, 43(8), 875-879, 1998.
- Sokolovskiy, S. V., Modeling and inverting radio occultation signals in the moist troposphere. *Radio Sci.*, 36(3), 441-458, 2001.

DANISH METEOROLOGICAL INSTITUTE

Scientific Reports

Scientific reports from the Danish Meteorological Institute cover a variety of geophysical fields, i.e. meteorology (including climatology), oceanography, subjects on air and sea pollution, geomagnetism, solar-terrestrial physics, and physics of the middle and upper atmosphere.

Reports in the series within the last five years:

No. 98-1

Niels Woetman Nielsen, Bjarne Amstrup, Jess U. Jørgensen:

HIRLAM 2.5 parallel tests at DMI: sensitivity to type of schemes for turbulence, moist processes and advection

No. 98-2

Per Høeg, Georg Bergeton Larsen, Hans-Henrik Benzon, Stig Syndergaard, Mette Dahl Mortensen: The GPSOS project

Algorithm functional design and analysis of ionosphere, stratosphere and troposphere observations

No. 98-3

Mette Dahl Mortensen, Per Høeg:

Satellite atmosphere profiling retrieval in a nonlinear troposphere
Previously entitled: Limitations induced by Multipath

No. 98-4

Mette Dahl Mortensen, Per Høeg:

Resolution properties in atmospheric profiling with GPS

No. 98-5

R.S. Gill and M. K. Rosengren

Evaluation of the Radarsat imagery for the operational mapping of sea ice around Greenland in 1997

No. 98-6

R.S. Gill, H.H. Valeur, P. Nielsen and K.Q. Hansen: Using ERS SAR images in the operational mapping of sea ice in the Greenland waters: final report for ESA-ESRIN's: pilot projekt no. PP2.PP2.DK2 and 2nd announcement of opportunity for the exploitation of ERS data projekt No. AO2..DK 102

No. 98-7

Per Høeg et al.: GPS Atmosphere profiling methods and error assessments

No. 98-8

H. Svensmark, N. Woetmann Nielsen and A.M. Sempreviva: Large scale soft and hard turbulent states of the atmosphere

No. 98-9

Philippe Lopez, Eigil Kaas and Annette Guldberg: The full particle-in-cell advection scheme in spherical geometry

No. 98-10

H. Svensmark: Influence of cosmic rays on earth's climate

No. 98-11

Peter Thejll and Henrik Svensmark: Notes on the method of normalized multivariate regression

No. 98-12

K. Lassen: Extent of sea ice in the Greenland Sea 1877-1997: an extension of DMI Scientific Report 97-5

No. 98-13

Niels Larsen, Alberto Adriani and Guido DiDonfrancesco: Microphysical analysis of polar stratospheric clouds observed by lidar at McMurdo, Antarctica

No.98-14

Mette Dahl Mortensen: The back-propagation method for inversion of radio occultation data

No. 98-15

Xiang-Yu Huang: Variational analysis using spatial filters

No. 99-1

Henrik Feddersen: Project on prediction of climate variations on seasonal to interannual timescales (PROVOST) EU contract ENVA4-CT95-0109: DMI contribution to the final report: Statistical analysis and post-processing of uncoupled PROVOST simulations

No. 99-2

Wilhelm May: A time-slice experiment with the ECHAM4 A-GCM at high resolution: the experimental design and the assessment of climate change as compared to a greenhouse gas experiment with ECHAM4/OPYC at low resolution

No. 99-3

Niels Larsen et al.: European stratospheric monitoring stations in the Arctic II: CEC Environment and Climate Programme Contract ENV4-CT95-0136. DMI Contributions to the project

No. 99-4

Alexander Baklanov: Parameterisation of the deposition processes and radioactive decay: a review and some preliminary results with the DERMA model

No. 99-5

Mette Dahl Mortensen: Non-linear high resolution inversion of radio occultation data

No. 99-6

Stig Syndergaard: Retrieval analysis and methodologies in atmospheric limb sounding using the GNSS radio occultation technique

No. 99-7

Jun She, Jacob Woge Nielsen: Operational wave forecasts over the Baltic and North Sea

No. 99-8

Henrik Feddersen: Monthly temperature forecasts for Denmark - statistical or dynamical?

No. 99-9

P. Thejll, K. Lassen: Solar forcing of the Northern hemisphere air temperature: new data

No. 99-10

Torben Stockflet Jørgensen, Aksel Walløe Hansen: Comment on "Variation of cosmic ray flux and global coverage - a missing link in solar-climate relationships" by Henrik Svensmark and Eigil Friis-Christensen

No. 99-11

Mette Dahl Meincke: Inversion methods for atmospheric profiling with GPS occultations

No. 99-12

Hans-Henrik Benzon; Laust Olsen; Per Høeg: Simulations of current density measurements with a Faraday Current Meter and a magnetometer

No. 00-01

Per Høeg; G. Leppelmeier: ACE - Atmosphere Climate Experiment

No. 00-02

Per Høeg: FACE-IT: Field-Aligned Current Experiment in the Ionosphere and Thermosphere

No. 00-03

Allan Gross: Surface ozone and tropospheric chemistry with applications to regional air quality modeling. PhD thesis

No. 00-04

Henrik Vedel: Conversion of WGS84 geometric heights to NWP model HIRLAM geopotential heights

No. 00-05

Jérôme Chenevez: Advection experiments with DMI-Hirlam-Tracer

No. 00-06

Niels Larsen: Polar stratospheric clouds micro-physical and optical models

No. 00-07

Alix Rasmussen: "Uncertainty of meteorological parameters from DMI-HIRLAM"

No. 00-08

A.L. Morozova: Solar activity and Earth's weather. Effect of the forced atmospheric transparency changes on the troposphere temperature profile studied with atmospheric models

No. 00-09

Niels Larsen, Bjørn M. Knudsen, Michael Gauss, Giovanni Pitari: Effects from high-speed civil traffic aircraft emissions on polar stratospheric clouds

No. 00-10

Søren Andersen: Evaluation of SSM/I sea ice algorithms for use in the SAF on ocean and sea ice, July 2000

No. 00-11

Claus Petersen, Niels Woetmann Nielsen: Diagnosis of visibility in DMI-HIRLAM

No. 00-12

Erik Buch: A monograph on the physical oceanography of the Greenland waters

No. 00-13

M. Steffensen: Stability indices as indicators of lightning and thunder

No. 00-14

Bjarne Amstrup, Kristian S. Mogensen, Xiang-Yu Huang: Use of GPS observations in an optimum interpolation based data assimilation system

No. 00-15

Mads Hvid Nielsen: Dynamisk beskrivelse og hydrografisk klassifikation af den jyske kyststrøm

No. 00-16

Kristian S. Mogensen, Jess U. Jørgensen, Bjarne Amstrup, Xiaohua Yang and Xiang-Yu Huang: Towards an operational implementation of HIRLAM 3D-VAR at DMI

No. 00-17

Sattler, Kai; Huang, Xiang-Yu: Structure function characteristics for 2 meter temperature and relative humidity in different horizontal resolutions

No. 00-18

Niels Larsen, Ib Steen Mikkelsen, Bjørn M. Knudsen m.fl.: In-situ analysis of aerosols and gases in the polar stratosphere. A contribution to THESEO. Environment and climate research programme. Contract no. ENV4-CT97-0523. Final report

No. 00-19

Amstrup, Bjarne: EUCOS observing system experiments with the DMI HIRLAM optimum interpolation analysis and forecasting system

No. 01-01

V.O. Papitashvili, L.I. Gromova, V.A. Popov and O. Rasmussen: Northern polar cap magnetic activity index PCN: Effective area, universal time, seasonal, and solar cycle variations

No. 01-02

M.E. Gorbunov: Radiographic methods for processing radio occultation data in multipath regions

No. 01-03

Niels Woetmann Nielsen; Claus Petersen: Calculation of wind gusts in DMI-HIRLAM

No. 01-04

Vladimir Penenko; Alexander Baklanov: Methods of sensitivity theory and inverse modeling for estimation of source parameter and risk/vulnerability areas

No. 01-05

Sergej Zilitinkevich; Alexander Baklanov; Jutta Rost; Ann-Sofi Smedman, Vasiliy Lykosov and Pierluigi Calanca: Diagnostic and prognostic equations for the depth of the stably stratified Ekman boundary layer

No. 01-06

Bjarne Amstrup: Impact of ATOVS AMSU-A radiance data in the DMI-HIRLAM 3D-Var analysis and forecasting system

No. 01-07

Sergej Zilitinkevich; Alexander Baklanov: Calculation of the height of stable boundary layers in operational models

No. 01-08

Vibeke Huess: Sea level variations in the North Sea – from tide gauges, altimetry and modelling

No. 01-09

Alexander Baklanov and Alexander Mahura: Atmospheric transport pathways, vulnerability and possible accidental consequences from nuclear risk sites: methodology for probabilistic atmospheric studies

No. 02-01

Bent Hansen Sass and Claus Petersen: Short range atmospheric forecasts using a nudging procedure to combine analyses of cloud and precipitation with a numerical forecast model

No. 02-02

Erik Buch: Present oceanographic conditions in Greenland waters

No. 02-03

Bjørn M. Knudsen, Signe B. Andersen and Allan Gross: Contribution of the Danish Meteorological Institute to the final report of SAMMOA. CEC contract EVK2-1999-00315: Spring-to.-autumn measurements and modelling of ozone and active species

No. 02-04

Nicolai Kliem: Numerical ocean and sea ice modelling: the area around Cape Farewell (Ph.D. thesis)

No. 02-05

Niels Woetmann Nielsen: The structure and dynamics of the atmospheric boundary layer

No. 02-06

Arne Skov Jensen, Hans-Henrik Benzon and Martin S. Lohmann: A new high resolution method for processing radio occultation data

No. 02-07

Per Høeg and Gottfried Kirchengast: ACE+: Atmosphere and Climate Explorer

No. 02-08

Rashpal Gill: SAR surface cover classification using distribution matching

No. 02-09

Kai Sattler, Jun She, Bent Hansen Sass, Leif Laursen, Lars Landberg, Morten Nielsen og Henning S. Christensen: Enhanced description

of the wind climate in Denmark for determination of wind resources: final report for 1363/00-0020: Supported by the Danish Energy Authority

No. 02-10

Michael E. Gorbunov and Kent B. Lauritsen:
Canonical transform methods for radio occultation data

No. 02-11

Kent B. Lauritsen and Martin S. Lohmann:
Unfolding of radio occultation multipath behavior using phase models

No. 02-12

Rashpal Gill: SAR ice classification using fuzzy screening method

No. 02-13

Kai Sattler: Precipitation hindcasts of historical flood events

No. 02-14

Tina Christensen: Energetic electron precipitation studied by atmospheric x-rays

No. 02-15

Alexander Mahura and Alexander Baklanov: Probabilistic analysis of atmospheric transport patterns from nuclear risk sites in Euro-Arctic Region

No. 02-16

A. Baklanov, A. Mahura, J.H. Sørensen, O. Rigina, R. Bergman:
Methodology for risk analysis based on atmospheric dispersion modelling from nuclear risk sites

No. 02-17

A. Mahura, A. Baklanov, J.H. Sørensen, F. Parker, F. Novikov K. Brown, K. Compton:
Probabilistic analysis of atmospheric transport and deposition patterns from nuclear risk sites in Russian Far East

No. 03-01

Hans-Henrik Benzon, Alan Steen Nielsen, Laust Olsen:
An atmospheric wave optics propagator, theory and applications